Polarized Absorption Spectra and Configuration Analyses of Xanthene and Xanthone

Tsuneyuki MINEGISHI, Toshihiko HOSHI,* Hiroshi HIRATSUKA, and Yoshie TANIZAKI

Department of Chemistry, Tokyo Institute of Technology, Meguro-ku, Tokyo 152

** Department of Chemistry, College of Science and Engineering, Aoyama Gakuin University, Chitosedai, Setagaya-ku, Tokyo 157*

(Received April 1, 1977)

The polarized absorption sepctra of xanthene and xanthone were measured in stretched poly(vinyl alcohol) films, and the polarization direction of each electronic transition was determined. It was confirmed that xanthone has the short molecular-axis polarized bands ($^1A_1 \leftarrow {}^1A_1$) at 343, 260, and 226 nm, and the long molecular-axis polarized ones ($^1B_2 \leftarrow {}^1A_1$) at 290, 266, and 242 nm. The electronic transitions of xanthone are discussed in connection with those of xanthene by use of the configuration analysis. For the 266 and 260 nm bands, the contributions of the intramolecular charge transfer character from the xanthene skeleton to the carbonyl group are considerable.

Derivatives of xanthone have been found as plant pigments and have received considerable attention because of their anomalous emission behavior. From lifetime and polarization measurements, it has been indicated that the configuration of the lowest triplet state of xanthone is $^3(n, \pi^*)$ type in a nonpolar solvent (3-methylpentane) but $^3(\pi, \pi^*)$ in a polar solvent.[1] The electronic absorption spectra of xanthone and its derivatives have been studied by several investigators,[1-3] but their assignments of the individual bands are different. For instance, Pownall and Huber[1] measured absorption and polarized phosphorescence spectra of xanthone, and they found five electronic bands at 364, 335, 282, 256, and 234 nm. The five bands were assigned to $^1A_2(n, \pi^*) \leftarrow {}^1A_1$, $^1A_1 \leftarrow {}^1A_1$, $^1B_2 \leftarrow {}^1A_1$, $^1A_1$–(CT)$\leftarrow {}^1A_1$, and $^1A_1 \leftarrow {}^1A_1$ transitions in order of increasing energy. From the measurements of absorption and fluorescence spectra and PPP calculations, Mizutani *et al.*[2] have also discussed the electronic structure of xanthone and its hydroxy and methoxy derivatives, and reported that there are a few discrepancies between their results and the above-mentioned ones.[1]

In this paper, measurements of polarized absorption spectra using stretched poly(vinyl alcohol) films and PPP calculations for xanthene and xanthone have been performed, and the electronic spectrum of xanthone is analyzed in connection with that of xanthene by use of the method of configuration analysis developed by Baba *et al.*[4]

Experimental

Materials. Commercially available (Tokyo Kasei Co., Ltd.) xanthene and xanthone were purified by repeated recrystallizations from ethanol. The melting point of xanthene was 99—100.2 °C (lit,[9] 99 °C) and that of xanthone 173.6 °C (lit,[9] 174 °C).

Measurements and Notations Used. The polarized absorption spectra were measured with a Shimadzu QV-50 spectrophotometer.[5-7]

The notations used in the figures of the polarized absorption spectra are as follows: R_s is a ratio of stretching,[5] $D_{//}$ and $D_\perp$ are absorbances for the light polarized parallel to and perpendicular to the stretched direction of the film, respectively, and R_d is the ratio of the optical densities ($R_d = D_{//}/D_\perp$).

In the case of planar molecules belonging to the point group C_{2v}, D_2, D_{2h} *etc.*, we can obtain a reduced polarization spectrum using the above-mentioned R_s and R_d values, *i.e.*, the absorption spectrum in a non-stretched polymer film can be reduced into two component spectra which are polarized parallel (D_z) to and perpendicular (D_y) to the principal symmetry axis (z).

Calculations

In the MO calculations, a modified PPP method developed by Nishimoto and Förster[8] was employed. The valence state ionization potentials ($I_p(r)$) and electron affinities ($E_a(r)$) used are as follows: $I_p(C) = 11.42$, $E_a(C) = 0.58$, $I_p(-O-) = 32.9$, $E_a(-O-) = 13.37$, $I_p(=O) = 23.7$, and $E_a(=O) = 2.47$ eV. The resonance integrals (β_{rs}) were adjusted at every iteration of the SCF calculations by the equations[8]

$$\beta_{CC} = -0.51 p_{CC} - 1.84,$$
$$\beta_{CO} = -0.56 p_{CO} - 2.20.$$

Here, p_{rs} is a π-bond order between the atoms r and s. In the CI calculations, all the one-electron excited configurations among the upper five occupied and lower five unoccupied SCF orbitals were taken into account.

It is very interesting for chemists to know the origin of the elctronic transitions more quantitatively. The configuration analysis developed by Baba and his coworkers[4] may be one of the most useful methods for this purpose. According to their method, any state function Ψ can be developed in terms of reference wavefunctions (Ψ°) appropriately chosen,

$$\Psi = \Psi^\circ M,$$

where M is a transformation matrix and the square of the matrix element (M_{ji}) of M represents the degree of contribution of a reference wavefunction Ψ_i° to the resultant wavefunction Ψ_j under consideration.

Results and Discussion

Figure 1 shows the polarized absorption spectrum of xanthene in the stretched poly(vinyl alcohol) film. The absorption spectrum ($D_{//}$ or $D_\perp$ curve) of this compound consists of three apparent bands at 294, 252, and ≈215 nm. The R_d values for the 252 nm band are large compared with those of the 294 nm band. This indicates that the relatively intense 252 nm band is polarized along the long molecular-axis (y-axis) and 294 nm

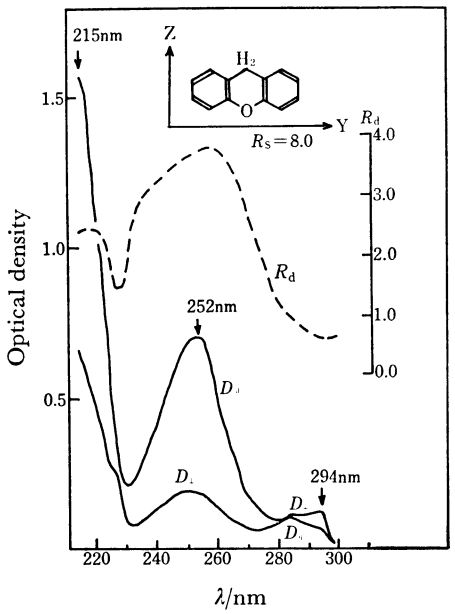

Fig. 1. The polarized absorption spectrum of xanthene in the stretched poly(vinyl alcohol) film.

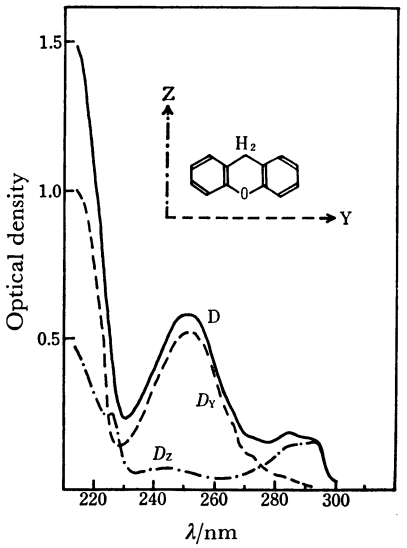

Fig. 2. The reduced polarized absorption spectrum of xanthene. D: The absorption spectrum in the non-stretched poly(vinyl alcohol) film. D_y and D_z: The reduced polarization spectrum.

band along the short-axis (z). The behavior of the R_d curve suggests the presence of additional weak bands at 285 and 226 nm, that is, the R_d values are steeply increased with decreasing wavelength around 285 nm and a distinct minimum is found at 226 nm. To determine in more detail the locations of these hidden bands, we obtained the reduced polarization spectrum, which is shown in Fig. 2. From this figure, it is clearly seen that the z-axis polarized bands are at 294 and 226 nm and the y-axis polarized ones are at 285, 252, and around 215 nm.

The above experimental results are compared with calculated ones in Table 1. From this table, it is clear that the observed 294 and 226 nm bands can be assigned

Table 1. Comparison of the observed and calculated transition energies, intensities, and polarizations for xanthene

Symmetry		Transition energy (nm)		Intensity		Polarization	
		Calcd	Obsd[a]	Calcd(f)	Obsd(ε)[b]	Calcd	Obsd
I	A_1	287	294	0.016	1900	z	z
II	B_2	287	285	0.008		y	y
III	B_2	254	252	0.500	8000	y	y
IV	A_1	222	226	0.001	*ca.* 6000	z	z
V	B_2	211	≈215	0.226	14700	y	y
VI	B_2	207		0.855		y	
VII	A_1	206		0.323		z	—

a) In poly(vinyl alcohol) film. b) In ethanol.

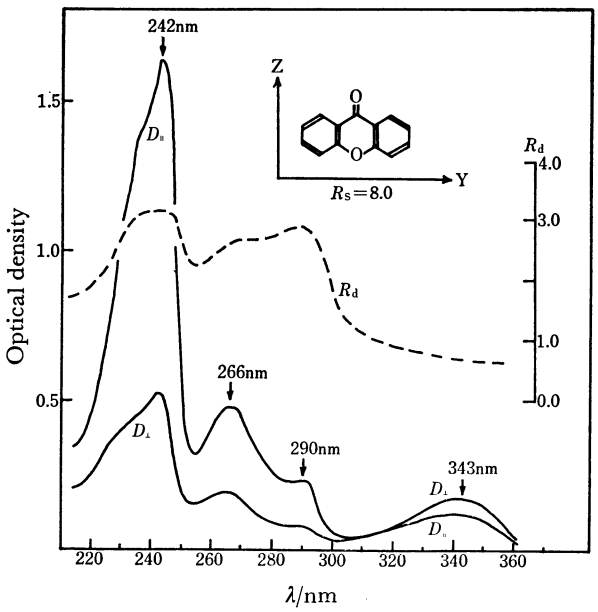

Fig. 3. The polarized absorption spectrum of xanthone in the stretched poly(vinyl alcohol) film.

to $^1A_1 \leftarrow {}^1A_1$ transitions and the observed 285 and 252 nm bands to $^1B_2 \leftarrow {}^1A_1$.

Figure 3 shows the polarized absorption spectrum of xanthone. The spectrum of this compound is very complex, *i.e.*, four apparent peaks are found at 343, 290, 266, and 242 nm besides a shoulder around 235 nm. The R_d curve shows clear maxima at 290 and 242 nm and a shoulder at 266 nm, indicating that the 290, 266, and 242 nm bands are polarized along the long molecular-axis (y). On the other hand, the 343 nm band is polarized along the short molecular-axis (z), because the R_d values for this band are the smallest in the observed wavelength region. The R_d values decrease steeply on both sides of the intense 242 nm band and a clear minimum is found around 254 nm. This indicates that weak bands polarized along the short molecular-axis are hidden at about 254 and 220 nm.

Figure 4 shows the reduced polarization spectrum of xanthone. From this figure the location of each band including above-mentioned hidden bands can be clearly seen. That is, the long molecular-axis polarized bands

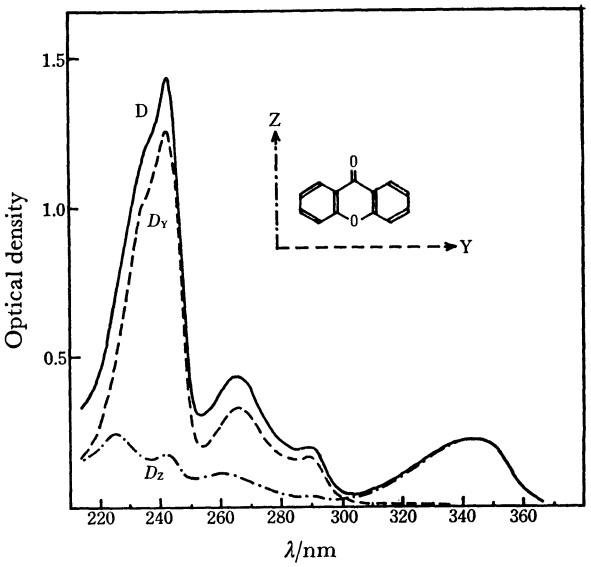

Fig. 4. The reduced polarized absorption spectrum of xanthone. Notations used: *cf.* Fig. 2.

are found at 290, 266, and 242 nm, and the short molecular-axis polarized ones at 343, 260, and 226 nm. From the above experimental results, the z-axis polarized 343 and 260 nm bands can be assigned to the $^1A_1 \leftarrow {}^1A_1$ transitions, and the y-axis polarized 290, 266, and 242 nm bands to $^1B_2 \leftarrow {}^1A_1$, as shown in Table 2. This assignment is not always consistent with the previously reported assignments.[1] For instance, the relatively intense 266 and 242 nm bands were earlier assigned to $^1A_1 \leftarrow {}^1A_1$ transitions.[1]

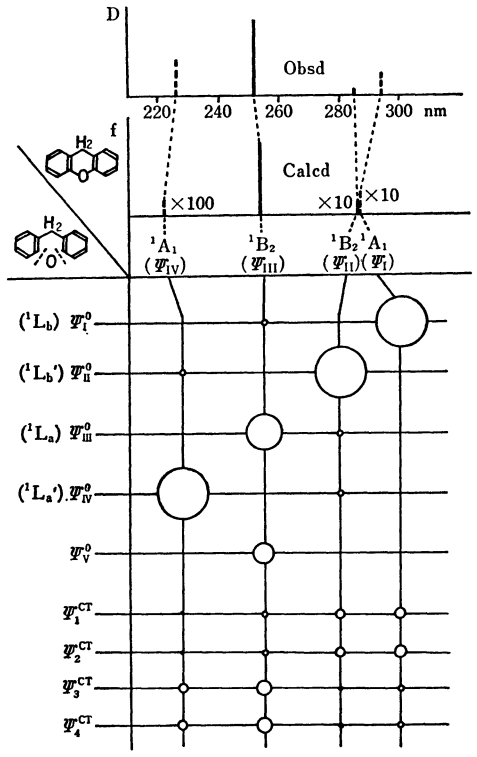

Fig. 5. Results of the configuration analysis of xanthene. The radius of the circle is proportional to the magnitude of M_{ji}, *i.e.* the area of the circle represents the degree of the contribution of Ψ_i^0 to Ψ_j.
D: Observed relative intensity.
f : Calculated oscillator strength.
Ψ_i^0 and Ψ_j: See text.
Ψ_i^{CT}: Wavefunction for the charge transfer state from oxygen to the two benzene rings.

TABLE 2. COMPARISON OF THE OBSERVED AND CALCULATED TRANSITION ENERGIES, INTENSITIES, AND POLARIZATIONS FOR XANTHONE

Sym-metry		Transition energy (nm)		Intensity		Polarization	
		Calcd	Obsd[a]	Calcd(f)	Obsd(ε)[b]	Calcd	Obsd
I	A_1	316	343	0.114	7200	z	z
II	B_2	293	290	0.003	4200	y	y
III	B_2	266	266	0.162	13000	y	y
IV	A_1	243	260	0.146		z	z
V	B_2	241	242	1.363	42800	y	y
VI	A_1	230	226	0.135		z	z
VII	B_2	228	—	0.027		y	—

a) In poly(vinyl alcohol) film. b) In ethanol.

Configuration Analysis. State wavefunctions of a molecule can be developed in terms of wavefunctions of an appropriately chosen reference molecule. In the case of xanthene, we have chosen the structure of the reference molecule as

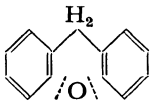

The results of the configuration analysis are shown in Fig. 5. From this figure, it is clear that the state wave-

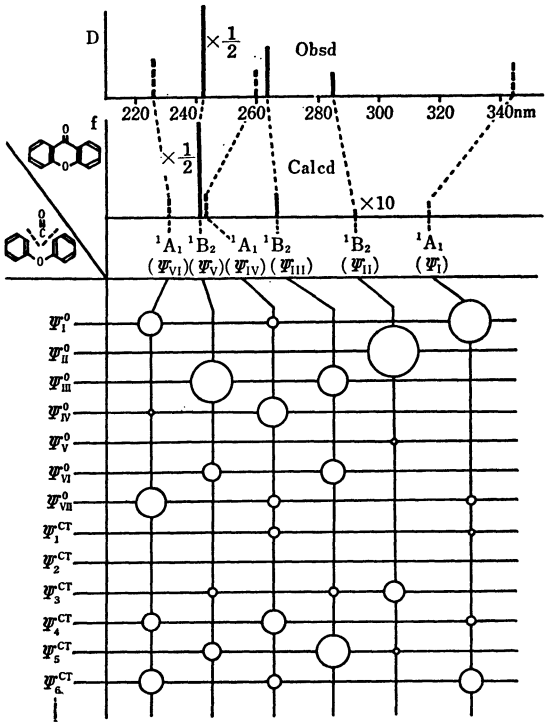

Fig. 6. Results of the configuration analysis of xanthone. See the explanation of Fig. 5, where Ψ_i^{CT} stands for wavefunction for the charge transfer state from xanthene skeleton to the carbonyl group.

functions Ψ_{I}, Ψ_{II}, Ψ_{III}, and Ψ_{IV} are approximately represented by the state functions Ψ_{I}°, Ψ_{II}°, Ψ_{III}°, and Ψ_{IV}° of the reference molecule, respectively. That is, it may be considered that the first two transitions ($\Psi_{I} \leftarrow \Psi_{0}$ and $\Psi_{II} \leftarrow \Psi_{0}$) arise from the interaction between the $^{1}L_{b}$ states of the two benzene rings and the next two transitions ($\Psi_{III} \leftarrow \Psi_{0}$ and $\Psi_{IV} \leftarrow \Psi_{0}$) from the two $^{1}L_{a}$ states.

As for xanthone, the excited state wavefunctions were developed in terms of the wavefunctions of xanthene (reference molecule) as shown in Fig. 6. The transitions I(Ψ_{I}), II(Ψ_{II}), and V(Ψ_{V}) of xanthone are approximately represented by the transitions I(Ψ_{I}°), II(Ψ_{II}°), and III(Ψ_{III}°), respectively. Transition III(Ψ_{III}) is considered to be due to the interaction of Ψ_{III}°, Ψ_{VI}°, and $\Psi_{CT_5}^{\circ}$, and transition IV(Ψ_{IV}) due to the interaction of Ψ_{IV}° and $\Psi_{CT_4}^{\circ}$, where Ψ_{CT}°'s represent the charge transfer configuration from the xanthene skeleton to the carbonyl group. Transitions III and IV of xanthone observed at 266 and 260 nm may be considered to be charge transfer bands. As for this molecule, charge transfer configurations from the C=O group to the xanthene skeleton can also be considered, but the contributions of these configurations are negligibly small.

References

1) H. J. Pownall and J. R. Huber, *J. Am. Chem. Soc.*, **93**, 6429 (1971).
2) K. Mizutani, K. Miyazaki, K. Ishigaki, and H. Hosoya, *Bull. Chem. Soc. Jpn.*, **47**, 1596 (1974).
3) A. A. Efimov, R. N. Nurmukhametov, I. L. Belaits, and A. I. Tolmachev, *Opt. Spectrosc.*, **30**, 337 (1971).
4) H. Baba, S. Suzuki, and T. Takemura, *J. Chem. Phys.*, **50**, 2078 (1969).
5) Y. Tanizaki, *Bull. Chem. Soc. Jpn.*, **38**, 1798 (1965).
6) T. Hoshi and Y. Tanizaki, *Z. Phys. Chem. (Frankfurt)*, **71**, 230 (1970).
7) T. Hoshi, H. Inoue, J. Shiraishi, and Y. Tanizaki, *Bull. Chem. Soc. Jpn.*, **44**, 1743 (1971).
8) K. Nishimoto and L. S. Förster, *Theor. Chim. Acta*, **3**, 407 (1969).
9) A. Albert, "Heterocyclic Chemistry," Athlone Press, London (1959), pp. 276—281.